RSC Advances

RSC Publishing

PAPER

View Article Online
View Journal | View Issue

Cite this: *RSC Advances*, 2013, **3**, 10786

Kinetic and thermodynamic study of 2′-hydroxy-8-methoxyflavylium. Reaction network interconverting flavylium cation and flavanone†

Vesselin Petrov,*[a] Ana Marta Diniz,[a] Luís Cunha-Silva,[b] A. Jorge Parola[a] and Fernando Pina[a]

Received 19th February 2013,
Accepted 11th April 2013

DOI: 10.1039/c3ra40846a

www.rsc.org/advances

2′-Hydroxyflavylium and 2′-hydroxyflavanone derivatives can be interconverted by a precise sequence of pH jumps, through the respective intermediate (mono) ionized *trans*-chalcones. In acidic and neutral media, the well known network of chemical reactions involving flavylium cation, quinoidal base, hemiketal, and *cis* and *trans* chalcones is established. In the pH range $8 < pH < 10$, the chalcone (**Ct**) deprotonates and evolves to the formation of a flavanone (**F**). At higher pH values, the di-ionized *trans*-chalcone is the stable species, formed from the flavylium cation. Acidification of the di-ionized *trans*-chalcone gives the flavylium cation or the flavanone, *via* the mono-ionized *trans*-chalcone, respectively at $pH < 1$ and $pH \approx 9$. In contrast with the chalcones, the flavanone once formed is stable even in acidic media. However, under strongly basic conditions, it leads back to the di-ionized *trans*-chalcone, the most stable species at more basic pH values, and the reactions leading to $\mathbf{Ct}^{-}$, **F**, $\mathbf{Ct}^{2-}$, $\mathbf{Ct}^{-}$, constitute a one direction cycle for interconversion of these species.

Introduction

Flavonoids are an important class of compounds playing important roles in plants life,[1] in human diet due to their beneficial effects such as anti-oxidants,[2] inhibition of the cholesterol absorption,[3] protection from ultra violet damage,[4] as well as in the pharmaceutical and cosmetic industries.[5] Polyphenols are also used to tan leather and are important constituents of wine in particular the red wine.[6] This work regards the interconversion between two relevant families of flavonoids, 2′-hydroxyflavylium cations and 2′-hydroxyflavanones, through 2,2′-dihydroxychalcone intermediates, Scheme 1.

Inspection of Scheme 1 indicates that it is possible to obtain from the common *trans*-2,2′-dihydroxychalcone intermediate, the corresponding 2′-hydroxyflavylium cation or the 2′-hydroxyflavanone, depending on pH and the nature of the *cis-trans* isomers. The interconversion between 2,2′-dihydroxychalcones and 2′-hydroxyflavanones requires ring closure/opening. In biological systems, the flavanone formation is catalyzed by the enzyme chalcone isomerase. In laboratory, this reaction can be achieved in the presence of bases[7] or light.[8] In spite of the numerous works regarding the chalcone-flavanone chemistry, the possibility of preparing 2,2′-dihydroxychalcones, which are able to switch from flavanone to flavylium cation by a sequence of defined pH jumps has been less explored.[9]

The aim of this work is to present a complete thermodynamic and kinetic study of 2′-hydroxy-8-methoxyflavylium chloride, Scheme 2, reporting the whole network of chemical reactions involving this molecule, determining the pH range where flavanone is formed and the possibility of reversibly interconvert the flavylium cation and the flavanone through a sequence of pH inputs.

Results and discussion

The network of chemical reactions of most flavylium derivatives is shown in Fig. 1. The flavylium cation, $\mathbf{AH}^{+}$, is stable only at pH values less than one, and by raising the pH to less acidic or neutral pH values, a sequence of reactions take place in different timescales: (i) the flavylium cation deprotonates to give the quinoidal base, **A**, in microseconds; (ii) the flavylium cation hydrates to form the hemiketal, **B**, in milliseconds to seconds depending on pH; (iii) the hemiketal ring opens through a tautomerization process leading to the *cis*-chalcone, **Cc**, in subseconds and finally; (iv) the *cis*-chalcone isomerizes

[a]*REQUIMTE, Departamento de Química, Faculdade de Ciências e Tecnologia, Universidade Nova de Lisboa, 2829-516 Monte de Caparica, Portugal. E-mail: v.petrov@fct.unl.pt*

[b]*REQUIMTE & Departamento de Química e Bioquímica, Faculdade de Ciências, Universidade do Porto, 4169-007 Porto, Portugal*

† Electronic supplementary information (ESI) available. CCDC 908022. For ESI and crystallographic data in CIF or other electronic format see DOI: 10.1039/c3ra40846a

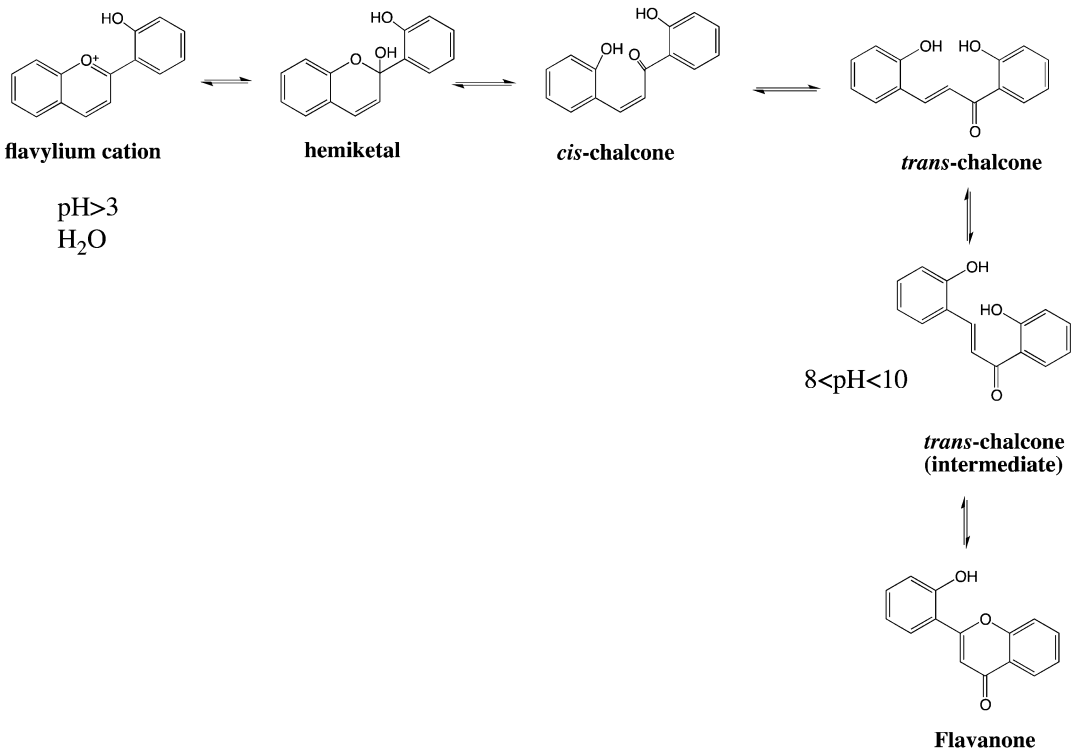

Scheme 1 Interconversion between 2′-hydroxyflavylium and 2′-hydroxyflavanone. The formation of a flavanone from a flavylium cation implies the presence of a hydroxyl group in position 2′ in the latter.

to the *trans*-chalcone in minutes to hours, depending on the isomerization kinetic barrier,[10] see Fig. 1.

As a result of these different timescales, after a direct pH jump from solutions of flavylium cation equilibrated at very acidic solutions (usually pH $\leqslant$ 1) to higher pH values, the quinoidal base is the first species to be formed. Dubois and Brouillard[11] proved that in the case of anthocyanins the quinoidal base, **A**, does not hydrate, unless by reaction with the hydroxide anion at basic pH values, and thus it is a kinetic product that evolves to **B** only through $\mathbf{AH}^+$. This behavior is also followed by many other flavylium derivatives.[12]

The study of the network is very simplified if eqn (1) is used to define an overall equilibrium. Eqn (1) is equivalent to a single acid–base equilibrium between flavylium cation and a conjugate base, **CB**, defined as the sum of the concentrations of the other species in the network,[11,13–15] [**CB**] = [**A**] + [**B**] + [**Cc**] + [**Ct**].

$$\mathbf{AH}^+ + H_2O \rightleftharpoons \mathbf{CB} + H_3O^+ \quad K'_a = K_a + K_h + K_hK_t + K_hK_tK_i \quad (1)$$

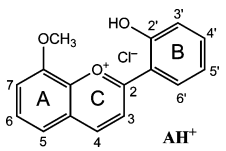

Scheme 2 2′-Hydroxy-8-methoxyflavylium chloride.

In the case of flavylium compounds bearing hydroxyl substituents, deprotonated quinoidal base and chalcone species are formed at higher pH values.[12]

The spectral variations accompanying the direct pH jumps from equilibrated solutions of 2′-hydroxy-8-methoxyflavylium

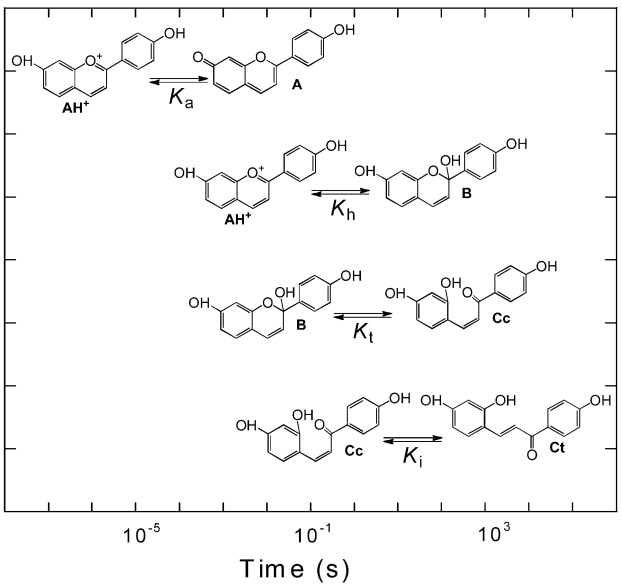

Fig. 1 Relative appearance time of the species involved in a typical flavylium reaction network, after a direct pH jump from 1 to the neutral pH region.

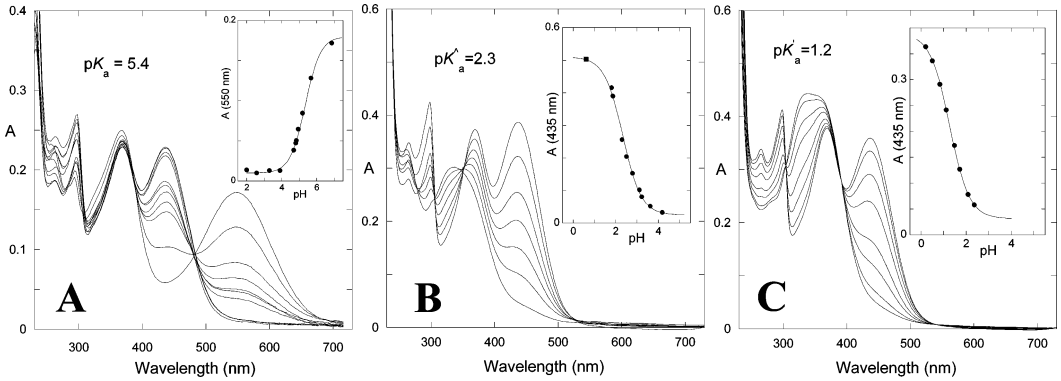

Fig. 2 A Absorption spectra of 5×10^{-5} M 2′-hydroxy-8-methoxyflavylium chloride at pH = 0.6 in acetonitrile: water 80 : 20 (v/v) taken 4.5 ms after pH jumps from pH = 0.6 to higher pH values, followed by stopped-flow; B The same as in A with 7.5×10^{-5} M after *ca.* 1 min, followed by UV-Vis spectroscopy; C The same as B after equilibration (*ca.* 8 h).[16]

chloride at pH = 0.6 in acetonitrile: water 80 : 20 (v/v) to higher pH values, taken 4.5 ms after the jump, 1 min after the pH jump and when the solutions are let to equilibrate over *ca.* 8 h are shown in Fig. 2.

After 4.5 ms, the data is compatible with a single acid–base equilibrium involving the flavylium cation, $\mathbf{AH}^+$ and the quinoidal base, **A**, with pK_a = 5.4, eqn (2). After *ca.* 1 min, a second (pseudo)equilibrium behaving as a single pseudo-acid–base system is observed with p$K\hat{}_a$ = 2.3, eqn (3). This kind of pseudo-equilibrium was previously described for anthocyanins and related compounds[12] and is attained between $\mathbf{AH}^+$, **A**, **B** and **Cc**, *i.e.*, all the species except **Ct** that takes much longer to equilibrate, eqn (3).

$$\mathbf{AH}^+ + H_2O \rightleftharpoons \mathbf{A} + H_3O^+ \qquad K_a = 10^{-5.4} \tag{2}$$

$$\mathbf{AH}^+ + H_2O \rightleftharpoons \mathbf{CB}\hat{} + H_3O^+ \qquad K\hat{}_a = 10^{-2.3} \tag{3}$$

Where

$$K\hat{}_a = \frac{[\mathrm{CB}\hat{}][H_3O^+]}{[\mathrm{AH}^+]} \tag{4}$$

$$[\mathbf{CB}\hat{}] = [\mathbf{A}] + [\mathbf{B}] + [\mathbf{Cc}] \tag{5}$$

and the equilibrium constant is defined by

$$K\hat{}_a = K_a + K_h + K_hK_t \tag{6}$$

The final equilibrium shown in Fig. 2C is reached between the flavylium cation, $\mathbf{AH}^+$, and all the basic species existing in the acidic-neutral region, as represented by eqn (1), $K'_a = K_a + K_h + K_hK_t + K_hK_tK_i = 10^{-1.2}$ (see Fig. S1 in ESI†). It is worthy of note the fact that depending on the nature of the substituents the mole fraction of the ''basic'' species **A**, **B**, **Cc** and **Ct**, can change dramatically: for example, in anthocyanins **B** is the major species, while in most synthetic flavylium compounds the predominant species in the equilibrium at neutral pH values is **Ct**.

In Fig. 2C, the raising of the absorption around 330 nm indicates that *trans*-chalcone should be formed, since this isomer exhibits higher mole absorption coefficients when compared with the *cis* analogue and is expected to absorb in this region of the spectrum. From the shape of the absorption bands it can not be excluded the existence of the hemiketal, **B**, after 1 min or at the equilibrium since this species should absorb in the UV region due to the disruption of the conjugation between the benzopyrylium ring and the phenyl ring caused by the existence of a sp^3 carbon in position 2.

In Fig. 3, the kinetic process during the first seconds after a direct pH jump from 0.6 to higher pH values, *i.e.* from the absorption spectra of Fig. 2A to Fig. 2B, are shown.

The direct pH jumps to the region $2 < \mathrm{pH} < 5$, as exemplified for pH = 2.6 in Fig. 3A, shows the conversion of the flavylium cation to give the species at the pseudo-equilibrium, hemiketal, **B**, and *cis*-chalcone **Cc**, followed by another, much slower, process to reach the equilibrium where **Ct** is the dominant species, see below Fig. 4.

In the case of a direct pH jump to the region $7 < \mathrm{pH} < 12$, the behavior is qualitatively similar as the one represented in Fig. 3B for pH = 9.3, the respective rate constants increasing with increasing pH. In contrast with the behavior of anthocyanins[1] and some flavylium derivatives,[12] the quinoidal base, **A**, formed from 2′-hydroxy-8-methoxyflavylium is very reactive and does not behave as a kinetic product. In a few seconds after the pH jump, it evolves to a mixture of hemiketal and chalcones,[17] the respective ratio depending on the pH. This process is followed by two other consecutive steps, the first one forming $\mathbf{Ct}^-$ and the second flavanone, see below.

The kinetic evolution from the pseudo-equilibrium to the equilibrium in acidic region is reported in Fig. 4. At pH = 2.2, Fig. 4A, the initial absorption spectrum is the one of the pseudo-equilibrium, where $\mathbf{AH}^+$, **B** and **Cc** are present which evolves to the final equilibrium, having **Ct** as the predominant species. Conversely, at pH = 3.6, Fig. 4B, the initial spectrum presents a small absorption due to the flavylium cation and the main absorption is due to **Cc**, which is transformed into **Ct**. Representation of the rate constants of the this process (the

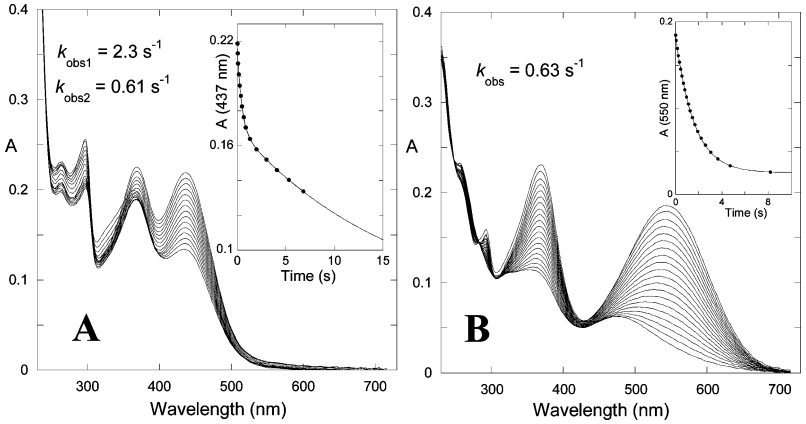

Fig. 3 A Spectral changes of the kinetic process following a pH jump from pH = 0.6 to 2.6; B The same as A after a pH jump from 0.6 to pH = 9.3.

slowest one in acidic pH) is shown in Fig. 4C. The shape of this curve is given by eqn (7). This equation is different from the one typically observed for flavylium derivatives lacking the *cis-trans* isomerization barrier,[18] because the quinoidal base, **A**, is not a kinetic product due to its very fast hydration. In eqn (7), the rate of **Ct** formation is the product of the mole fraction distribution of **Cc** multiplied by the isomerization constant considering also the back reaction. At pH values near neutrality, the *cis* and the *trans*-chalcone deprotonate and these deprotonated species isomerize faster, not only because $\mathbf{Cc}^-$ is now the major species at the pseudo-equilibrium but also the isomerization constant k'_i tends to increase.[19,22]

$$k_{obs} = \chi_{Cc}k_i + k_{-i} + \chi_{Cc^-}k'_i + k'_{-i} \quad (7)$$

$$\chi_{Cc} = \frac{K_h K_t}{[H^+] + K_a + K_h + K_h K_t} \quad (8)$$

$$\chi_{Cc^-} = \frac{\chi_{Cc} K_{Cc/Cc^-}}{[H^+]} \quad (9)$$

A very interesting feature of the present system, reported in Fig. 5, is the possibility of obtaining a flavanone from the $\mathbf{Cc}^-$/$\mathbf{Ct}^-$ species. The first spectrum after a pH jump to 8.2 (bold line) corresponds to the spectrum of the pseudo-equilibrium, mainly **Cc**/$\mathbf{Cc}^-$. The initial raising of the absorption is compatible with the formation of **Ct**/$\mathbf{Ct}^-$, as observed for more acidic pH values: from this point onwards the absorption starts to decrease and the final spectrum, traced line, is attributed to the formation of a new species (see Scheme 3). From a more concentrated solution equilibrated at pH $\approx$ 9, it was possible to isolate a solid sample whose ^{1}H NMR ($CDCl_3$) data confirms the presence of both *trans*-2,2′-dihydroxy-3′-methoxychalcone (**Ct**) and 2′-hydroxy-3′-methoxyflavanone (**F**). The former is characterized by the presence of two doublets at 7.92 and 8.13 ppm with a large coupling constant (15.7 Hz) as expected for a *trans* double C=C bond while the latter is characterized by the presence of three high field signals centered at 2.98. 3.06 and 5.87 ppm corresponding to the aliphatic protons 2, 3a and 3b (see ESI† for full characterization). From the NMR tube, single crystals appro-

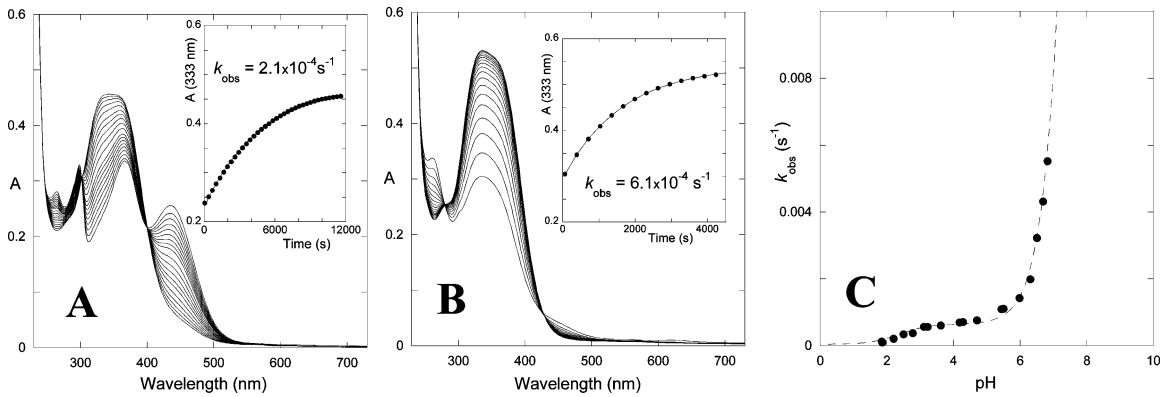

Fig. 4 Spectral changes accompanying the slowest process in reaching equilibrium upon direct pH jumps: A direct pH jump from pH = 0.6 to pH = 2.2; B direct pH jump from pH = 0.6 to pH = 3.6; C pH dependence of the observed rate constant of the slowest step; fitting with eqn (7) was achieved for pK_a = 5.4, pK_{Cc/Cc^-} = 7.9, k_i = 7.5 $\times$ 10^{-4} s^{-1}, k'_i = 0.068 s^{-1}, the reverse reactions are neglected due to the relatively smaller values of these constants (k_{-i} and k'_{-i}).

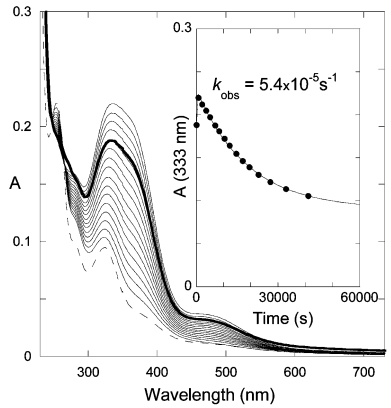

Fig. 5 Spectral changes after a pH jump from 0.6 to 8.2; Bold line spectrum immediately (*ca.* 1 min) after pH the jump; Traced line spectra of the flavanone species obtained after final equilibration (*ca.* 48 h).

priate for X-ray diffraction analysis could be isolated that revealed to be **Ct**.

The solid-state structure of the compound *trans*-2,2′-dihydroxy-3′-methoxychalcone (**Ct**) was unveiled in the triclinic crystal system (space group $P\bar{1}$) with the asymmetric unit cell revealing only a single **Ct** molecule (detailed information about the crystallographic data collection and structure refinement are in experimental section). The structure reveals high planarity with the two phenyl rings practically in the same plane (the dihedral angle between the average planes of these two aromatic groups is *ca.* 0.68(4)°). This planarity was previously observed in other *trans*-2′-hydroxychalcones, *e.g.*, (*E*)-1-(2-hydroxy-4-methoxyphenyl)-3-(2,3,4-trimethoxyphenyl)-prop-2-en-1-one[20] and (*E*)-3-(2,3-dimethoxyphenyl)-1-(2-hydroxy-4-methoxyphenyl)prop-2-en-1-one,[21] being largely conditioned by the strong intra- and intermolecular O–H···O hydrogen bonds (Fig. 6A and 7b). In fact, **Ct** shows a strong intramolecular hydrogen bond interaction O1–H1···O2 [distances H1···O2 and O1···O2 of 1.635(12) Å and 2.5439(15) Å, respectively; angle (O1 H1 O2) of 154.3(17)°] and adjacent **Ct** molecules connect by intermolecular hydrogen bonds of type O3–H6···O2^{i} [distances H1···O2 and O1···O2 of 1.915(11) Å and 2.7847(14) Å, respectively; angle (O6 H3 O2^{i}) of 154.8(16)°; symmetry operation: (i) $-x$, $-y$ + 2, $-z$ + 1] leading to the formation of dimeric supramolecular entities in an anti-parallel arrangement (rotated by *ca.* 180°; Fig. 6B). The 2′-OH group appears to be critical for the observed planarity since chalcones lacking such hydroxyl group present large dihedral angles between rings A and B; *trans*-4-acetyl-7-diethylamino-2-hydroxychalcone ((*E*)-1-(4-acetylphenyl)-3-(4-diethylamino)-2-hydroxyphenyl)prop-2-en-1-one), for instance, has a dihedral angle of 35°.[9] Furthermore, contiguous **Ct** molecules are closely packed along the *a*-axis of the unit cell through off-set π···π stacking interactions involving the aromatic rings [C_g···C_g distances of 3.6627(3) and 3.67150(3) Å; C_g stands for the gravity center of the phenyl rings], ultimately leading to a global 3D supramolecular network (Fig. 6C).

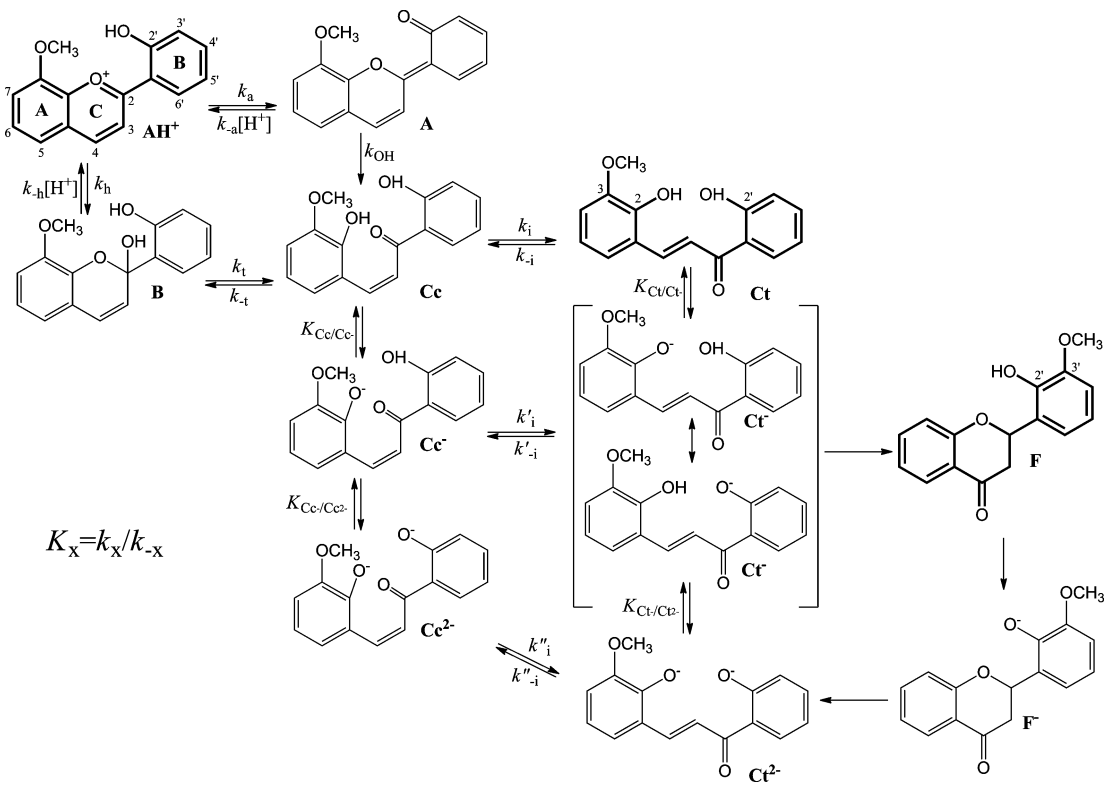

Scheme 3 Network of chemical reactions shown by 2′-hydroxy-8-methoxyflavylium.

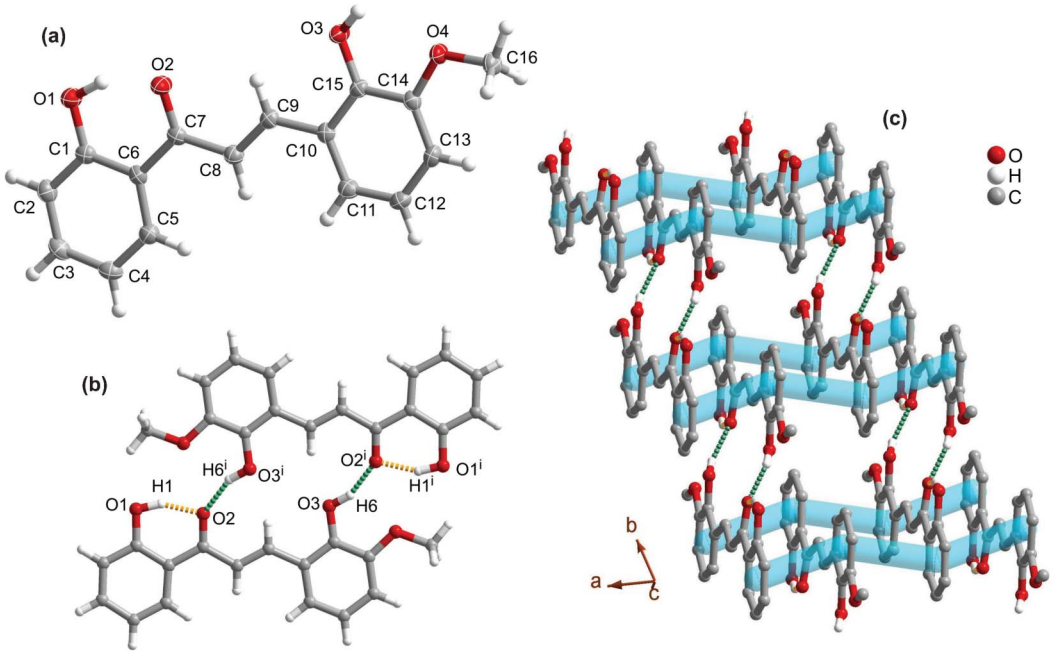

Fig. 6 (a) Crystal structure of **Ct** showing the label scheme for all non-H-atoms; C- and O-atoms represented as thermal ellipsoids drawn at the 50% probability level and H-atoms as small spheres with arbitrary radius. (b) Supramolecular dimer with the intra- and intermolecular O–H···O hydrogen bonds represented ad golden and green dashed lines, respectively. (c) Crystal packing, highlighting the stacking by π···π contacts (transparent blue tubes) between the aromatic rings along the a-axis of the unit cell.

The formation of the flavanone from $\mathbf{Ct}^-$ occurs only in a rather narrow pH window, 8 < pH < 10, as also reported for the compound 2′-hydroxyflavylium tetrafluoroborate.[22] For pH > 10, the di-ionized species $\mathbf{Ct}^{2-}$ starts to form and this is the more stable species at higher pH values. A series of pH jumps from a solution equilibrated at pH = 13 (100% $\mathbf{Ct}^{2-}$) to lower pH values permits determination of the two pK_a's of Ct, Fig. 7A, and the absorption spectra of **Ct**, $\mathbf{Ct}^-$ and $\mathbf{Ct}^{2-}$, Fig. 7B, as well the respective mole fraction distribution of species, Fig. 7C. It is worth of mention the pH dependence of the flavanone rate formation, which follows the mole fraction distribution of $\mathbf{Ct}^-$ in the range 8 < pH < 10, Fig. 7C. At 10 < pH < 12, the process is more complex since Ct^- originates both flavanone and $\mathbf{Ct}^{2-}$; for pH > 12 no flavanone is formed.

Reverse pH jumps from fresh solutions (in the pseudo-equilibrium) at moderately acidic pH values to more acidic conditions could give relevant information about the network, Fig. 8.[23] Considering that the pseudo-equilibrium at moderately acidic pH values involves the species **A**, **B** and **Cc**, a reverse pH jump back to strongly acidic media would involve three steps: (i) very fast conversion of all **A** in $\mathbf{AH}^+$ (too fast to be observed by stopped-flow); (ii) formation of more $\mathbf{AH}^+$ from **B**, a fast process at these pH values since the hydration-dehydration reaction is proportional to the proton concentration, and (iii) formation of even more $\mathbf{AH}^+$ from **Cc**, through **B**.

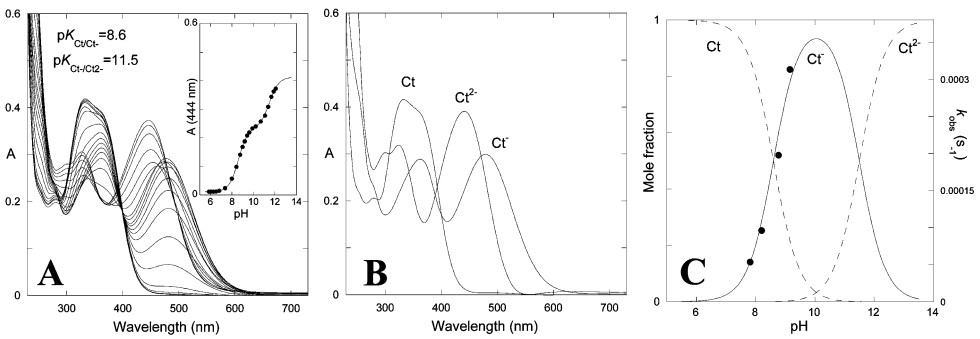

Fig. 7 A Spectral changes corresponding to the titration of $\mathbf{Ct}^{2-}$ from pH 12 to lower pH values; inset: fitting of the data at 444 nm yields pK_{Ct/Ct^-} = 8.6 and pK_{Ct/Ct^-} = 11.5; B individual spectra of the **Ct**, $\mathbf{Ct}^-$ and $\mathbf{Ct}^{2-}$ species; C mole fraction distribution of species; black circles represent the rate of flavanone formation.

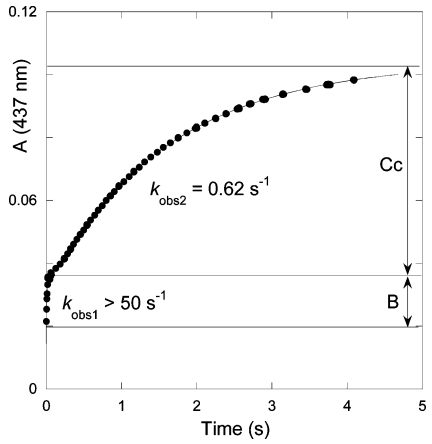

Fig. 8 Reverse pH jump from a fresh solution of 2′-hydroxy-8-methoxyflavylium chloride at pH = 4.02 back to pH = 1.33; K_t = 1.8; k_t = 1.1 s^{-1}; k_{-t} = 0.62 s^{-1}.

The kinetic trace in Fig. 8 could be fitted with two exponentials, whose amplitude ratio is equal to the tautomerization equilibrium constant, K_t, Fig. 8.

Having determined K_t (Fig. 8), K_a and $K\hat{}_a$ (Fig. 1), the value of K_h = 1.8 × 10^{-3} M could be calculated using eqn (6). Using then eqn (1) and the value of K_a (Fig. 1), the isomerization constant K_i = 18 could also be calculated. The thermodynamic constants for the chemical reaction network originated in solution by 2′-hydroxy-8-methoxyflavylium chloride are shown in Table 1, together with kinetic data. Several kinetic constants of the system (see Scheme 3) were determined. The kinetic data of Fig. 8 permits to obtain k_{-t} = 0.62 s^{-1} and from K_t, k_t = 1.1 s^{-1}. The kinetic data from Fig. 4C gives the value of k_i = 7.5 × 10^{-4} s^{-1} and from the respective equilibrium constant, k_{-i} = 4.2 × 10^{-5} s^{-1}. The kinetic data in Fig. 3A allows calculation of the kinetic constants for the hydration step: since $k_{obs1} = k_h + k_{-h}[H^+]$ = 2.3 s^{-1} and $K_h = k_h/k_{-h}$ the values of k_h and k_{-h} are obtained.

The thermodynamic data in Table 1 can be used to build an energy-level diagram describing the chemical reaction network of the present flavylium compound, Scheme 4. Under very acidic conditions, the flavylium cation **AH**$^+$ is the more stable species. Upon a pH jump to pH values in the neutral region, the quinoidal base **A** is formed as a kinetic product and then evolves (through **AH**$^+$) to a mixture of **B** and **Cc**. This mixture constitutes the pseudo-equilibrium ($K\hat{}_a$) which is established in the timescale of seconds to a few minutes. In the timescale of hours the system evolves to the final thermodynamic equilibrium (K'_a), where **Ct** is the predominant species at neutral pH values. A pH jump to pH values in the basic region leads to the formation of **Ct**/**Ct**$^-$/**Ct**$^{2-}$ depending on pH (through **A**, **Cc**, **Cc**$^-$ and **Cc**$^{2-}$). If the pH is in the range 8 < pH < 10, the final equilibrium includes also flavanone **F** besides the *trans*-chalcones.

Table 1 Thermodynamic and kinetic data for 2′-hydroxy-8-methoxyflavylium chloride in water/acetonitrile 80 : 20 (v/v)

pK_a	5.4 ± 0.1	k_h	0.93 ± 0.08 s^{-1}
p$K\hat{}_a$	2.3 ± 0.07	k_{-h}	535 ± 17 M^{-1} s^{-1}
pK'_a	1.2 ± 0.08	k_t	1.8 ± 0.2 s^{-1}
K_h	(1.8 ± 0.2) × 10^{-3} M	k_{-t}	0.62 ± 0.05 s^{-1}
K_t	1.8 ± 0.2	k_i	(7.5 ± 0.2) × 10^{-4} s^{-1}
K_i	18 ± 0.2	k_{-i}	(4.2 ± 0.1) × 10^{-5} s^{-1}
pK_{Cc/Cc^-}	7.9 ± 0.08		
pK_{Ct/Ct^-}	8.6 ± 0.08		
p$K_{Ct^-/Ct^{2-}}$	11.5 ± 0.1		

Conclusions

The chemistry of flavylium cation is very rich, since depending on pH, a reversible network of chemical reactions takes place, forming: (i) quinoidal bases (when hydroxyl substituents are present), (ii) hemiketal, (iii) *cis* and *trans* chalcones. The thermodynamic and kinetics of this network of chemical reactions involving the compound 2′-hydroxy-8-methoxyflavylium chloride was studied in detail and the respective energy level diagram constructed. In the present compound, the existence of an hydroxyl in position 2′ of the flavylium cation, allows formation of the ionized *trans*-2,2′-dihydroxy-3-methoxychalcone, which is transformed into 2′-hydroxy-3′-methoxyflavanone in the range 8 < pH < 10. The flavylium flavanone interconversion is possible by a sequence of pH and time stimuli. After a pH jump from 1 to 8 < pH < 10 the flavylium is transformed into the *trans*-chalcone, which in a few hours at room temperature gives the respective flavanone. The flavanone is stable upon a pH jump to acidic medium. On contrary, basification of the flavanone to pH = 12 leads to the fast formation of the de-ionized *trans*-chalcone. Acidification of this last species can give flavylium cation or the other species of the flavylium network, according to the final pH.

The chalcone-flavanone chemistry has been reported in some extent. However, the extension of the system to include the flavylium cation through 2,2′-dihydroxychalcones has received much less attention. The work here described opens a new synthetic route to obtain new substituted 2′-hydroxy-

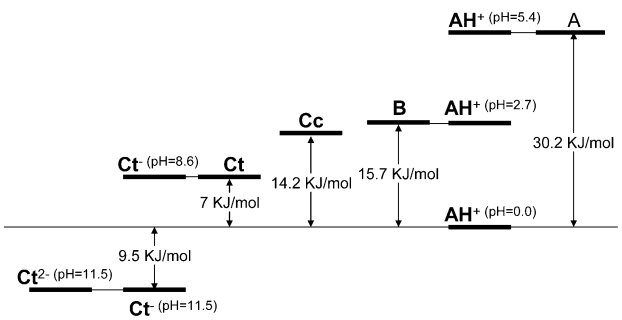

Scheme 4 Energy-level diagram for the chemical reaction network of 2′-hydroxy-8-methoxyflavylium chloride in water/acetonitrile 80 : 20 (v/v).

flavanones, which are relatively rare, from the adequate 2′-hydroxyflavylium derivatives.

Experimental

General for synthesis and spectroscopic characterization. All solvents and chemicals employed for synthesis and for preparation of samples were of reagent or spectrophotometric grade and were used as received; Millipore grade water was used. NMR spectra were run on a Bruker AMX 400 instrument operating at 400.13 MHz (^{1}H) and 100.00 MHz (^{13}C). Elemental analyses were performed in a Thermofinnigan Flash EA 112 series. Mass spectra were run on an Applied Biosystems Voyager-DE™ PRO. The pH of the solutions was adjusted by addition of HCl, NaOH or universal buffer of Theorell and Stenhagen[24] and pH was measured in a Radiometer Copenhagen PHM240 pH/ion meter. UV-Vis absorption spectra were recorded in a Varian-Cary 100 Bio or 5000 spectrophotometer. Spectroscopic experiments were carried out in buffered water/acetonitrile 80 : 20 (v/v) solutions. UV/Vis absorption spectra were recorded with a Varian-Cary 100 Bio spectrophotometer or in a Shimadzu VC2501-PC. The stopped flow experiments were conducted in an Applied Photophysics SX20 stopped-flow spectrometer provided with a PDA.1/UV photodiode array detector.

Synthesis of 2-(2′-hydroxyphenyl)-8-methoxy-1-benzopyrylium chloride 2′-hydroxy-8-methoxyflavylium chloride), ***AH***$^+$. 3-Methoxysalicylaldehyde (1.52 g, 10 mmol) and 2′-hydroxyacetophenone (1.36 g, 10 mmol) were dissolved in 6 ml of formic acid. The solution was saturated with dry hydrogen chloride for 2.5 h.[25] By the following day, diethyl ether was added and a red solid precipitated out. The solid was filtered off, carefully washed with diethyl ether and dried. The solid was recrystallized dissolving in methanol containing a few drops of HCl and letting diethyl ether gently diffuse (0.37 g, 1.3 mmol). Yield: 13%. ^{1}H and ^{13}C NMR (D_2O/DCl, pD ~ 1): see ESI† for full assignment. MS-MALDI/TOF(+): calcd for $C_{16}H_{13}O_3^+$: m/z (%) 253.09 (100); found: 253.10 $[M]^+$ (100). Elemental Analysis: calcd for $C_{16}H_{13}ClO_3$ (%) C 66.56, H 4.54; found: C 66.26; H 4.47.

Isolation of trans-2,2′-dihydroxy-3-methoxychalcone ((*E*)-1-(2-*hydroxyphenyl*)-3-(2-*hydroxy-8-methoxyphenyl*)*prop-2-en-1-one*), ***Ct***. 4′-Hydroxy-8-methoxyflavylium chloride (50 mg) was dissolved in a mixture of water and acetonitrile (4 : 1) and the pH adjusted to 8. By the following day, a yellow solid had precipitated from the solution that was filtered off, washed with water and dried. ^{1}H and ^{13}C NMR ($CDCl_3$): see ESI† for full assignment. MS-MALDI/TOF(−): calcd for $C_{16}H_{14}O_4$: m/z (%) 270.09 (100); found: 268.89 $[M - H]^-$ (100). Elemental Analysis: calcd for $C_{16}H_{13}ClO_3$ (%): C 71.10; H 5.22; found: C 71.16; H 5.32.

Characterization of 2′-hydroxy-3′-methoxyflavanone (2-(2-*hydroxy-3-methoxyphenyl*) *chroman-4-one*), ***F***. 2′-Hydroxy-8-methoxyflavylium chloride (50 mg) was dissolved in a mixture of water and ethanol (1 : 1) and the pH adjusted to 9.0. By the following day, the ethanol had mostly evaporated and a light yellow solid precipitated from the aqueous solution. The solid was filtered off, washed with water and dried. ^{1}H and ^{13}C NMR ($CDCl_3$) show the presence of Ct and flavanone (see ESI† for full NMR characterization of each species). From the NMR tube, single crystals appropriate for X-ray diffraction analysis could be isolated that revealed to be **Ct**.

Single-crystal X-ray diffraction. A single-crystal of the compound **Ct** was manually harvested and mounted on a on a Hampton Research CryoLoop using FOMBLIN Y perfluoropolyether vacuum oil (LVAC 25/6), with the assistance of a stereomicroscope.[26] Diffraction data were collected at 150(2) K on a Bruker X8 Kappa APEX II Charge-Coupled Device (CCD) area-detector diffractometer controlled by the APEX2 software package[27] (Mo-Kα graphite-monochromated radiation, λ = 0.71073 Å; crystal positioned at 35 mm from the detector and 60 s of exposure time) and equipped with an Oxford Cryosystems Series 700 monitored remotely with the software interface Cryopad.[28] Images were processed with the software SAINT+,[29] and absorption correction was executed by the multi-scan semi-empirical method implemented in SADABS.[30] The structure was solved by the direct methods employed in SHELXS-97,[31,32] with all the non-H-atoms located from difference Fourier maps calculated by successive full-matrix least-squares refinement cycles on F^2 using SHELXL-97,[32,33] and successfully refined with anisotropic displacement parameters. H-atoms associated to carbons were located at their idealized geometric positions using appropriate *HFIX* instructions in SHELXL, 43 for the H-atoms of CH groups and 137 for the Hs of the methyl group. Afterwards, were included in the subsequent refinement cycles in riding-motion approximation with isotropic thermal displacements parameters (U_{iso}) fixed at 1.2 and 1.5 × U_{eq} of the carbon atom to which they are attached, respectively. H-atoms of the hydroxyl groups were markedly visible in the difference Fourier maps, and included in subsequent refinement stages with the O–H distances restrained to 0.95(1), and using a riding-motion approximation with an isotropic thermal displacement parameter fixed at 1.5 × U_{eq} of the parent O-atom.

Information concerning the crystallographic data collection and structure refinement of ***Ct***: $C_{16}H_{14}O_4$, M = 270.27; triclinic, $P\bar{1}$; a = 7.1190(5) Å, b = 7.4620(5) Å, c = 12.5730(9) Å, α = 76.093(3)°, β = 85.589(3)°, γ = 73.234(3)°, V = 620.74(7) Å^3; T = 150(2)K; Z = 2; μ = 0.104 mm^{-1}; ρ_c = 1.446 g cm^{-3}; yellow plate crystal with 0.15 × 0.10 × 0.02 mm^3; 8835 reflections measured with 2334 being independent (R_{int} = 0.0281); the final R_1 and $wR(F^2)$ values were 0.0380 [$I > 2\sigma(I)$] and 0.0988 (all data), respectively; data completeness to θ = 25.68°, 99.3%.

Acknowledgements

This work was supported by Fundação para a Ciência e Tecnologia through the National Portuguese NMR Network, grant PEst-C/EQB/LA0006/2011 and project PTDC/QUI-QUI/119932/2010.

References

1 FLAVONOIDS: Chemistry, Biochemistry, and Applications, Edited by Øyvind M. Andersen and Kenneth R. Markham, 2006, CRC Press, Taylor & Francis Group, ISBN 0-8493-2021-6.
2 P. G. Pietta, *J. Nat. Prod.*, 2000, **63**, 1035–1042.
3 Y. Arai, S. Watanabe, M. Kimira, K. Shimoi, R. Mochizuki and N. Kinae, *J. Nutr.*, 2000, **130**, 2243–2250.
4 A. Kootstra, *Plant Mol. Biol.*, 1994, **26**, 771–774.
5 J. Arct and K. Pytkowska, *Clin. Dermatol.*, 2008, **26**(4), 347–57.
6 R. Corder, W. Mullen, N. Q. Khan, S. C. Marx, E. G. Woods, M. J. Carrier and A. Crozier, *Nature*, 2006, **444**, 566.
7 R. Mondal, A. Das Gupta and A. K. Mallik, *Tetrahedron Lett.*, 2011, **52**, 5020–5024, and references cited therin.
8 M. Sisa, S. L. Bonnet, D. Ferreira and J. H. Van der Westhuizen, *Molecules*, 2010, **15**, 5196–5245.
9 S. Gago, V. Petrov, A. M. Diniz, A. J. Parola, L. Cunha-Silva and F. Pina, *J. Phys. Chem. A*, 2012, **116**, 372–380.
10 A. Roque, J. C. Lima, A. J. Parola and F. Pina, *Photochem. Photobiol. Sci.*, 2007, **6**, 381–385.
11 R. Brouillard and J.-E. Dubois, *J. Am. Chem. Soc.*, 1977, **99**, 1359–1364.
12 F. Pina, M. J. Melo, C. A. T. Laia, A. J. Parola and J. C. Lima, *Chem. Soc. Rev.*, 2012, **41**, 869–908.
13 R. Brouillard and B. Delaporte, *J. Am. Chem. Soc.*, 1977, **99**, 8461–8468.
14 R. Brouillard, B. Delaporte and J.-E. Dubois, *J. Am. Chem. Soc.*, 1978, **100**, 6202–6205.
15 R. Brouillard and J. Lang, *Can. J. Chem.*, 1990, **68**, 755–761.
16 After long time storage the solutions show some discoloration at low pH values and slow precipitation at neutral pH values.
17 The light intensity of the stopped flow instrument is very intense and may convert partially some Cc into Ct.
18 F. Pina, V. Petrov and C. A. T. Laia, *Dyes Pigm.*, 2012, **92**, 877–889.
19 V. Petrov, R. Gomes, A. J. Parola and F. Pina, *Dyes Pigm.*, 2009, **80**, 149–155.
20 A. S. Pandi, D. Velmurugan, S. S. S. Raj, H. K. Fun and M. C. Bansal, *Acta Crystallogr., Sect. C: Cryst. Struct. Commun.*, 2003, **59**, O302–O304.
21 C. A. Escobar, A. Vega, D. Sicker and A. Ibanez, *Acta Crystallogr., Sect. E: Struct. Rep. Online*, 2008, **64**, O1834–O1834.
22 V. Petrov, R. Gomes, A. J. Parola, A. Jesus, C. A. T. Laia and F. Pina, *Tetrahedron*, 2008, **64**, 714–720.
23 R. A. McClelland and S. Gedge, *J. Am. Chem. Soc.*, 1980, **102**, 5838–5848.
24 F. W. Küster and A. Thiel, Tabelle per le Analisi Chimiche e Chimico-Fisiche, 12nd ed, 1982, Hoepli, Milano, pp. 157–160.
25 R. Robinson and F. M. Irvine, *J. Chem. Soc.*, 1927, 2086–2094.
26 T. Kottke and D. Stalke, *J. Appl. Crystallogr.*, 1993, **26**, 615–619.
27 APEX2, *Data Collection Software Version 2.1-RC13, Bruker AXS*, Delft, The Netherlands, 2006.
28 Cryopad, *Remote monitoring and control, Version 1.451*, Oxford Cryosystems, Oxford, United Kingdom, 2006.
29 SAINT+, *Data Integration Engine v. 7.23a* ©, 1997–2005, Bruker AXS, Madison, Wisconsin, USA.
30 G. M. Sheldrick, *SADABS v.2.01, Bruker/Siemens Area Detector Absorption Correction Program*, 1998, Bruker AXS, Madison, Wisconsin, USA.
31 G. M. Sheldrick, *SHELXS-97, Program for Crystal Structure Solution*, University of Göttingen, 1997.
32 G. M. Sheldrick, *Acta Crystallogr., Sect. A: Found. Crystallogr.*, 2007, **64**, 112–122.
33 G. M. Sheldrick, *SHELXL-97, Program for Crystal Structure Refinement*, University of Göttingen, 1997.

